



**HAL**  
open science

## A novel colorimetric and fluorescent turn-on pH sensor with a notably large Stokes shift for its application

Yaoyao Ning, Xiaoqing Wang, Kangjia Sheng, Lili Yang, Wei Han, Chaoni Xiao, Jianli Li, Yongmin Zhang, Shaoping Wu

► **To cite this version:**

Yaoyao Ning, Xiaoqing Wang, Kangjia Sheng, Lili Yang, Wei Han, et al.. A novel colorimetric and fluorescent turn-on pH sensor with a notably large Stokes shift for its application. *New Journal of Chemistry*, 2018, 42 (17), pp.14510-14516. 10.1039/C8NJ02860E . hal-01909358

**HAL Id: hal-01909358**

**<https://hal.sorbonne-universite.fr/hal-01909358>**

Submitted on 31 Oct 2018

**HAL** is a multi-disciplinary open access archive for the deposit and dissemination of scientific research documents, whether they are published or not. The documents may come from teaching and research institutions in France or abroad, or from public or private research centers.

L'archive ouverte pluridisciplinaire **HAL**, est destinée au dépôt et à la diffusion de documents scientifiques de niveau recherche, publiés ou non, émanant des établissements d'enseignement et de recherche français ou étrangers, des laboratoires publics ou privés.

# A novel colorimetric and fluorescent turn-on pH sensor with a notably large Stokes shift for its application

Yaoyao Ning,<sup>a,b,§</sup> Xiaoqing Wang,<sup>c,§</sup> Kangjia Sheng,<sup>a,b</sup> Lili Yang,<sup>a,b</sup> Wei Han,<sup>a</sup> Chaoni Xiao,<sup>a</sup> Jianli Li,<sup>c</sup> Yongmin Zhang<sup>a,b,d</sup> and Shaoping Wu<sup>a,b,\*</sup>

A novel naked-eye colorimetric and fluorescent turn-on pH sensor based on naphthalenone scaffold was rationally designed and facilely synthesized. The probe exhibited strong alkaline pH-dependent ( $pK_a=9.92$ ) behavior, high selectivity, sensitivity, high quantum efficiency ( $\Phi=0.64$ ) and rapid respond to pH fluctuations (within 1 min) in the range of 9.0 - 14.0. In addition, probe **DDTM** displayed a notably large Stokes shift of 198 nm. The response mechanism of the fluorescent probes was proposed to be caused by OH<sup>-</sup>-induced structure changes from the nonfluorescent **DDTM** form to the highly emissive addition product (more than 150-fold fluorescence enhancement) along with ICT changes. Live cell imaging data revealed that probe **DDTM** could selectively monitor pH changes with low cytotoxicity and cell membrane permeability. Therefore, this probe could be acted as an effective intracellular pH imaging sensor under extreme alkaline condition in the biomedical and biological fields.

## 1. Introduction

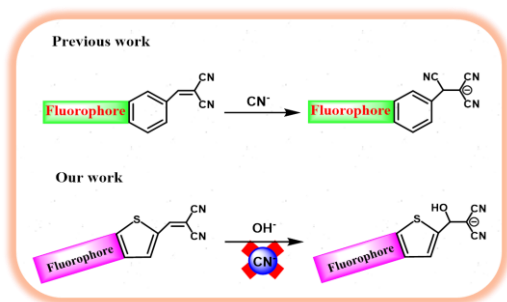
It is well known that the pH values are uniquely of high importance among the few chemical parameters. Specially, intracellular pH plays an important role in cell function and regulation such as cell volume regulation [1], vesicle trafficking, cellular metabolism [2], cell membrane polarity [3], cellular signalling, cell activation, growth, proliferation and apoptosis [4]. As an important indicator of cellular health, abnormal pH values of intracellular could lead to cellular functional disorders and serious diseases such as cancer [5,6], stroke [7], Alzheimer's disease [8], neurodegenerative disorders [9] and cardiovascular disease [10]. Therefore, it is extremely crucial to sense and monitor pH changes in living cells for investigating cellular functions and further providing insight into physiological and pathological processes.

A variety of analytical techniques have been reported to measure pH value including acid-base indicator titration [11], potentiometric titration [12], nuclear magnetic resonance [13], Raman sensor [14] and so on. Hence, it is essential for the health professional to have simple and effective methodologies for the rapid, selective, and sensitive detection of pH values in biological specimens. Fluorescent probes have been found widespread application for sensing and imaging pH values in living cells and tissues due to its high sensitivity, easy operation, real-time and noninvasive imaging properties [15]. However, a lot of reported pH probes still have some drawbacks such as low fluorescence quantum yields, poor photostability and narrow Stokes shifts. For the sake of overcoming these drawbacks, it is important to develop new longwave fluorescent probes with large Stokes shifts, and high turn-on fluorescence brightness.

Naphthalenone derivatives have been found to exhibit a variety of biological activities [16,17] and have also been surveyed for their suitability as dyes scaffold [18,19]. In addition, aromatic heterocyclic compounds containing a five-

membered furan or thiophene unit have been extensively studied in recent years due to their impressive optical properties and excellent charge-transport properties [20,21]. Therefore, construction of naphthalenone derivatives containing heterocyclic unit will be vital in synthesis of novel organic materials with appealing photonic and electronic functionality.

As part of our ongoing program in the study of novel fluorescent dyes [22,23], in the current work, a novel pH-response fluorescent probe **DDTM** was rationally designed and facilely synthesized by connecting a **DTC** fluorophore and a dicyanomethylidene group with double bond. In **DDTM**, the dicyanomethylidene group was used as an acceptor moiety while the amino group acts as an electron donor to form push-pull system. This probe displayed that ICT was conjugated organic  $\pi$ -systems with acceptor and donor subunits. To our surprise, the dicyanomethylidene group of probe **DDTM**, one of cyanide receptors, has no reaction with cyanide ion except OH<sup>-</sup> [24]. Compared with other reported pH probes [25-32], probe **DDTM** exhibited strong pH-dependent behaviour, high selectivity, sensitivity and responded linearly and rapidly to respond pH fluctuations within the range of 9.0 - 14.0. Specially, probe **DDTM** displayed a notably large Stokes shift of 198 nm and high fluorescence quantum yields. The response mechanism of the fluorescent probes could be caused by the OH<sup>-</sup>-induced structure changes from the nonfluorescent **DDTM** form to the highly emissive addition product along with ICT changes. Furthermore, live cell imaging data revealed that probe **DDTM** could selectively monitor pH changes with low cytotoxicity. Therefore, this probe could be used to visualize extreme alkaline within the biomedical and biological fields (Scheme 1).



**Scheme 1.** Strategies to response of pH probe.

## 2. Materials and methods

### 2.1. Materials

All chemical reagents were purchased from commercial suppliers and used without further purification. All organic solvents used for this work were of analytical grade also without further purification. All reaction processes were monitored through thin layer chromatography (TLC) which was performed by using Merck F254 gel-60 plates. Silica gel (200 mesh) was used as the solid phase for column chromatography by Qingdao Ocean Chemicals (China). All metal ions were prepared from corresponding salts. All samples were prepared at room temperature before UV-vis and fluorescence determination. The phosphate-buffered saline (PBS) was prepared from sodium dihydrogen phosphate and disodium hydrogen phosphate. Probe standard solution dissolved in DMSO and diluted to 50 mL volumetric flask. Distilled water was prepared from a Millipore water purification system. All glassware was cleaned with ultrapure water for three times and dried before use.

### 2.2. Instrumentation and methods

A pH meter (Sartorius PB-10) was used to determine the pH value. UV-vis absorption spectra were measured at room temperature with a Shimadzu UV-2550 spectrophotometer in 1 cm quartz. The fluorescence spectra were taken on a Hitachi F-7000 Fluorescence spectrophotometer (Hitachi, Japan) using a 5.0 nm slit width in a 1×1 cm quartz cell. The cells fluorescence imaging was obtained by laser scanning confocal fluorescence microscopy Olympus FV1000 (Olympus Corporation, Tokyo, Japan). High resolution mass spectra (HRMS) were recorded on a micro TOF-QII mass spectrometer. <sup>1</sup>H NMR and <sup>13</sup>C NMR spectra were obtained by Varian Gemini 2000 DMX600 MHz FT NMR spectrometers using CDCl<sub>3</sub>/DMSO-*d*<sub>6</sub> as solvent and TMS as internal standard. The chemical shifts were represented by ppm. The quantum yield was measured at room temperature referenced to Quinine sulphate dehydrates in aqueous solution of 0.1 M sulfuric acid. The structures of synthesized compounds were characterized by HRMS, <sup>1</sup>H NMR, <sup>13</sup>C NMR and the related spectra are shown in the Supplementary Information.

### 2.3. Synthesis of compound 2- ((7- (dimethylamino) -4,5 -dihydronaphtho [1,2-b] thiophen - 2-yl) methylene) malononitrile (DDTM)

A solution of **DTC** [33] (0.0500 g, 0.19 mmol, 1.0 equiv.) and malononitrile (0.0130 g, 0.19 mmol, 1.0 equiv.) in anhydrous CH<sub>2</sub>Cl<sub>2</sub> (5 mL) was treated with triethylamine (0.2 mL) at room temperature under argon. The reaction mixture was stirred at room temperature for 3 h. The solvent was evaporated under reduced pressure, and the residue was purified by silica gel column chromatography. (Yield: 40.5%, R<sub>f</sub> = 0.5, PE: EtOAc= 3:1). <sup>1</sup>H NMR (600 MHz, CDCl<sub>3</sub>) δ 7.58 (s, 1H), 7.45 (s, 1H), 7.36 (d, J = 8.5 Hz, 1H), 6.62-6.48 (m, 2H), 3.04 (s, 6H), 2.96-2.87 (m, 2H), 2.81 (dd, J = 23.5, 16.5 Hz, 2H). <sup>13</sup>C NMR (151 MHz, CDCl<sub>3</sub>) δ 152.53, 151.97, 149.76, 139.29, 138.62, 136.61, 131.25, 130.63, 126.94, 118.68, 114.93, 111.54, 71.69, 40.62, 32.28, 30.39, 30.06, 23.90. HRMS (C<sub>18</sub>H<sub>15</sub>N<sub>3</sub>S): calcd. for [M+H]<sup>+</sup> 306.1059; found: [M+H]<sup>+</sup> 306.0987.

### 2.4. Titration experiments of probe DDTM

For UV-vis and fluorescence titrations, stock solution of probe **DDTM** (1.0 mM) was prepared in DMSO solution. Different portions of the stock solution were then diluted to different concentrations for further usage. Generally, 50 μL of probe **DDTM** solution was added into 5 mL of buffer solution (10 mM PBS buffer, 20% DMSO) in a colorimetric tube. The other ions were dissolved in deionized water and added to the probe solution under the same condition. The pH variations of the solution were adjusted by adding the different volumes of NaOH (0.1 M or 1.0 M). The resulting solution was shaken well and incubated for 5 min at room temperature before measurements. The spectra of these solutions were recorded by means of fluorescence method. Fluorescence measurements were carried out with a slit width of 5 nm (λ<sub>ex</sub> = 380 nm) in 10 mm quartz cuvettes at room temperature and the scan rate was 1200 nm/min.

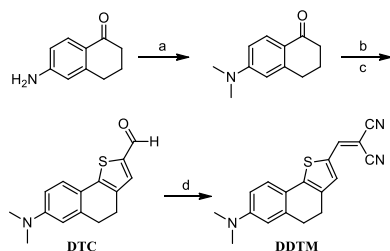
### 2.5. Cytotoxicity experiments

HeLa cells were purchased from the ATCC Cell Bank. Cell counting kit-8 (CCK-8) was used to detect the cytotoxicity of probe **DDTM**. Cells were seeded in 96-well plates at a concentration of 2 × 10<sup>4</sup> cells per well and cultured for 24 h in DMEM (supplemented with 10% fetal bovine serum (FBS)) in an incubator (37 °C 5% CO<sub>2</sub>). After the cells were incubated with probe **DDTM** at different concentrations (0, 5, 10, 15, 20 and 25 μM) for 24 h, CCK-8 (10 μL) was added to each well of the 96-well plate for 3 h at 37 °C the absorbance was measured at 450 nm using a microplate reader. Five replicates were done for each treatment group.

### 2.6. Cell imaging of probe DDTM

HeLa cells were placed on a 20 mm diameter glass bottomed culture dish and allowed to adhere for 24 h for intracellular imaging of OH<sup>-</sup>. Before confocal scanning imaging, these cells were incubated with 10 μM of probe **DDTM** at 37 °C for 30 min followed by washing three times with phosphate-buffered saline (PBS, pH = 7.4). Subsequently, the cells were washed with PBS for three times to remove excess **DDTM**, then in situ treated with different pH value solution (pH 10.0 and 12.0,

respectively), cells were then visualized with a FV1000 laser scanning confocal microscope. The excitation wavelength was set to 405 nm and 543 nm.



Reagents and Conditions: (a)  $\text{CH}_3\text{I}$ ,  $\text{K}_2\text{CO}_3$ , DMF,  $50^\circ\text{C}$  24 h, 54%; (b)  $\text{POCl}_3$ , DMF,  $90^\circ\text{C}$  reflux 5 h; (c)  $\text{Na}_2\text{S} \cdot 9\text{H}_2\text{O}$ , Chloroacetaldehyde,  $\text{K}_2\text{CO}_3$ , DMF, 42% in two steps; (d) Malononitrile,  $\text{Et}_3\text{N}$ ,  $\text{CH}_2\text{Cl}_2$ , R.T. 3 h, 41%.

**Scheme 2.** Synthesis of probe **DDTM**.

### 3. Results and discussion

#### 3.1. Synthesis of probe DDTM

The general synthetic route of probe **DDTM** was shown in **Scheme 2**. **DTC** was conveniently synthesized according to our previous work. Then **DTC** reacted with malononitrile to obtain the probe **DDTM** by Knoevenagel condensation at moderate yield in one step. The structure of probe **DDTM** was characterized and confirmed by  $^1\text{H}$  NMR,  $^{13}\text{C}$  NMR and HRMS data.

#### 3.2. Photophysical properties of probe DDTM

Probe **DDTM** exhibited good solubility in common organic solvents such as  $\text{CH}_2\text{Cl}_2$ ,  $\text{CHCl}_3$ , THF and DMSO. On one hand, probe **DDTM** was slightly soluble in water but DMSO could help increase its water solubility. On the other hand, the respond of probe **DDTM** toward  $\text{OH}^-$  has the maximum fluorescence emission wavelength in DMSO solvent (**Fig. S1**). So DMSO was preferred to be co-solvent in the photophysical properties experiment. In addition, the maximum emission wavelength of probe **DDTM** toward  $\text{OH}^-$  was obtained in PBS buffer (**Fig. S2**). Hence, probe **DDTM** could dissolve completely in a mixture of DMSO/PBS buffer (10 mM PBS buffer, 20% DMSO) and the corresponding solution exhibited an efficient fluorescent turn on mode for pH value change within 1 minute. The colour of probe **DDTM** in a mixture of DMSO/PBS buffer pH 7.4 was light pink with a distinct absorption band at 430 nm. On the contrary, the colour of the mixture was changed from light pink to yellow and the absorbance of probe **DDTM** drastically increases at 430 nm when pH value increased to 11.0 (**Fig. S3**). The change of colour was readily observed by naked-eye.

In addition, no emission wavelength of probe **DDTM** was appeared from 450 nm to 650 nm with the fluorescence quantum efficiency of 0.01 (Quinine sulphate dehydrate in 0.1 M  $\text{H}_2\text{SO}_4$  was used as the main standard,  $\Phi_s = 0.54$ ,  $\lambda_{\text{ex}} = 365$  nm). The low quantum efficiency was occurred by ICT process from the amino group of naphthalenone scaffold as an electron acceptor group to the dicyanovinyl moiety as an electron acceptor group by its  $\pi$ -conjugation. To our delight,

the remarkable fluorescence enhancement was observed more than 150-fold and the quantum efficiency increased to 0.64 due to the disruption of ICT phenomena of probe **DDTM** when pH value increased to 11.0, the fluorescence colour was changed from colourless to orange to yellow with the maximum emission wavelength at 578 nm. The dicyanovinyl group could be modulated by reacting with  $\text{OH}^-$ , and this nucleophilic addition reaction could finally interrupt the  $\pi$ -conjugation leading to the turn on mode of this detection.

#### 3.3. UV-vis absorbance and fluorescence response of probe DDTM to pH

The UV-Vis and fluorescence properties of probe **DDTM** were measured in a mixture of DMSO/PBS buffer system (10 mM PBS buffer, 20% DMSO) for detecting pH changes. As shown in **Fig. 1(a)**, the absorbance at 430 nm was gradually increased and had a good linear relationship with pH value in the range from 10.5 to 13.5 ( $R^2 = 0.9946$ ) along with the pH value increase. At the same time, the solution colour was drastically changed from light pink to yellow accompanied with these absorption changes. So probe **DDTM** could be used as naked-eye-visible pH indicators in aqueous media due to their sensitive colour response to solution pH change.

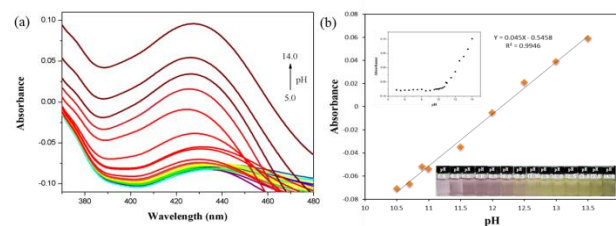


**Fig. 1.** (a) UV-Vis absorption spectra of probe **DDTM** (10  $\mu\text{M}$  in 10 mM PBS buffer, 20% DMSO) in accurate pH values ranging from 5.0 to 14.0 at  $25^\circ\text{C}$ . (b) Linear relationship of UV-Vis absorption at 430 nm and pH values from 10.5 to 13.5. Inset: the colour of probe **DDTM** in the different pH values under daylight lamp.

Further for fluorescent responses, as depicted in **Fig. 2**, probe **DDTM** itself had no fluorescence intensity at 578 nm, however, the fluorescence intensity increased with a concomitant enhancement in pH changes. With the variation of pH from 8.0 to 14.0, the probe showed turn-on fluorescence. Notably, a good linearity ( $R^2 = 0.9958$ ) between the fluorescence intensities with pH in the range of 9.5- 10.7 was obtained, the regression equation was  $Y = 2324.5X - 21250$ . Additionally, on the basis of the Henderson-Hasselbalch equation ( $\log [(I_{\text{max}} - I) / (I - I_{\text{min}})] = \text{pH} - \text{pK}_a$ ), the  $\text{pK}_a$  value of probe **DDTM** was determined to be 9.92 by analysis of the dependency of fluorescence intensities at 578 nm (**Fig. 3**). These results demonstrated that probe **DDTM** could be used to detect pH value quantitatively in extreme alkaline solution.

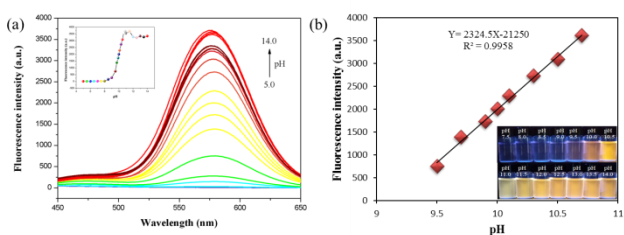


**Fig. 2.** (a) Emission spectra of probe **DDTM** (10  $\mu$ M in 10 mM PBS buffer, 20% DMSO) in accurate pH values ranging from 5.0 to 14.0 at 25  $^{\circ}$ C ( $\lambda_{\text{ex}}$ =380 nm, slit: 5.0 nm/5.0 nm). Inset: Fluorescence intensity at 578 nm by pH values according to the fluorescence titration (pH 5.0~14.0). (b) The linear relationship of fluorescence intensity at 578 nm and pH values from 9.5 to 10.7. Inset: the color of probe **DDTM** in the different pH values under UV 365 nm.

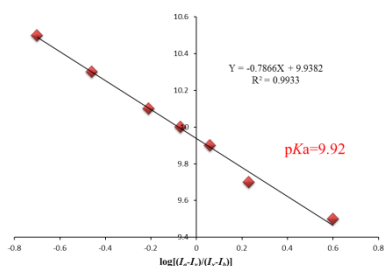


**Fig. 3.** Linear regression relationship between the pH value and  $\log \left[ \frac{(F_{\text{max}} - F_x)}{(F_x - F_{\text{min}})} \right]$ .

### 3.4. Selectivity experiment of probe **DDTM** to pH

The intracellular environment is quite complex and many biological molecules are present, such as amino acids, cysteine (Cys), homocysteine (Hcy) and glutathione (GSH), metal ions and reactive oxygen species (ROS) and so on. In order to verify whether these biomolecules could disturb the pH measurement efficiently in living cells, the selectivity of **DDTM** to alkaline over these species was investigated at pH 11.0, the results were shown in **Fig. 4(a)**, metal ions and reactive oxygen species showed very weak fluorescence intensity at 578 nm. In contrast, the strong fluorescence signal of probe **DDTM** was observed at 578 nm in alkaline solutions. Meanwhile, all biomolecules of fluorescence response in neutral and alkaline environments were evaluated to survey competition experiments. As shown in **Fig. 4(b)**, addition of biomolecules has no interference on the fluorescent spectroscopic changes to pH under the testing conditions. All these results indicated that probe **DDTM** could serve as a highly selective chemosensor for pH change in extreme alkaline solution.

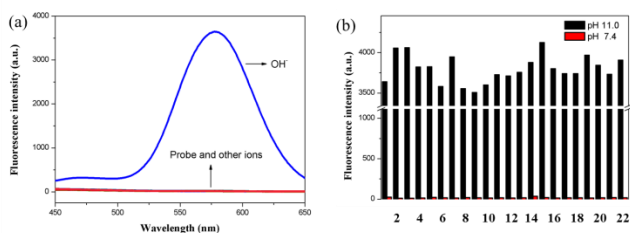


**Fig. 4.** (a) Emission spectra of probe **DDTM** in the presence of different metal ions and biologically relevant analytes (10  $\mu$ M) in the pH 11.0 solution. (b) Fluorescence respond of probe **DDTM** (10  $\mu$ M) in the presence of different metal ions and biologically relevant analytes 1.0 mM in the two pH values. 1: Blank; 2:  $\text{AcO}^-$ ; 3:  $\text{ClO}_4^-$ ; 4:  $\text{CO}_3^{2-}$ ; 5:  $\text{ClO}^-$ ; 6:  $\text{NO}_3^-$ ; 7:  $\text{ONOO}^-$ ; 8:  $\text{SO}_3^{2-}$ ; 9: Cys; 10: GSH; 11:  $\text{H}_2\text{O}_2$  (0.5 mM); 12:  $\text{Ba}^{2+}$ ; 13:  $\text{Ca}^{2+}$ ; 14:  $\text{CN}^-$ ; 15:  $\text{Cu}^{2+}$ ; 16:  $\text{Fe}^{3+}$ ; 17:  $\text{Hg}^{2+}$ ; 18:  $\text{K}^+$ ; 19:  $\text{Mg}^{2+}$ ; 20:  $\text{Na}^+$ ; 21: DTT; 22:  $\text{H}_2\text{S}$ . ( $\lambda_{\text{ex}}$ =380 nm, slit: 5.0 nm/5.0 nm).

### 3.5. Time-dependent effect and reversibility study of probe **DDTM**

The time-dependent course analysis showed that probe **DDTM** could quickly respond to pH value change for less than one minute at pH 11.0. As shown in **Fig. 5(a)**, after addition of **DDTM** to PBS buffer solutions at pH 7.4 and 11.0 at room temperature, respectively, the fluorescence intensity of the probe instantly reached equilibrium and remained unchanged for at least 30 min. The experimental results proved that probe **DDTM** has rapid respond to pH changes in extreme alkaline solution.

As for pH probes, the reversibility was one of the vital requirements for practical applications. Therefore, the reversibility of probe **DDTM** was explored that the pH value of the solution was switched back and forth between pH 4.0 and 11.0 using concentrated hydrochloric acid and aqueous sodium hydroxide. As shown in **Fig. 5(b)**, probe **DDTM** exhibited a highly reversible response to pH and the response time in different pH values were less than 10 s. Switching between the fluorescence on/off states could be repeated along with the colour change repeatedly between colourless (pH 4.0) and yellow (pH 11.0). These results demonstrated that probe **DDTM** could show quick and reversible responses to pH changes, and also be potentially useful to real-time monitor pH value changes in extreme alkaline solution.

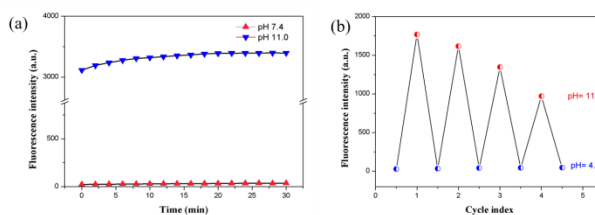


**Fig. 5.** (a) Time course of fluorescence intensity of probe **DDTM** (10  $\mu$ M in 10 mM PBS buffer, 20% DMSO) in the two pH values. (b) pH reversibility of probe **DDTM** (10  $\mu$ M in 10 mM PBS buffer, 20% DMSO) between pH 4.0 and pH 11.0 at 25  $^{\circ}$ C ( $\lambda_{\text{ex}}$ =380 nm, slit: 5.0 nm/5.0 nm).

### 3.6. Proposed detection mechanism and theoretical computation

The mechanism for the fluorescence enhancement of probe **DDTM** was proposed as shown in **Fig. 6**. In alkaline solution, hydroxyl ion reacted as nucleophilic reagent on the double bond of dicyanovinyl group in probe **DDTM** to give the addition intermediate, which could finally interrupt the  $\pi$ -conjugation leading to produce strong fluorescence. Then

hydroxyl of the addition intermediate could be occurred in protonation process in acid condition, finally probe **DDTM** is regenerated and the water molecule is released. To further confirm the proposed detection mechanism of probe **DDTM** towards hydroxyl, probe **DDTM** was reacted with tetrabutyl ammonium hydroxide at room temperature for 10 min in MeOH solution, then the reaction solution was diluted appropriately and tested by mass spectroscopy, an expected signal at  $m/z$  322.9321 corresponding to addition intermediate [probe **DDTM** + OH]<sup>-</sup> was observed (Fig. S4), and these data were consistent with the proposed mechanism.

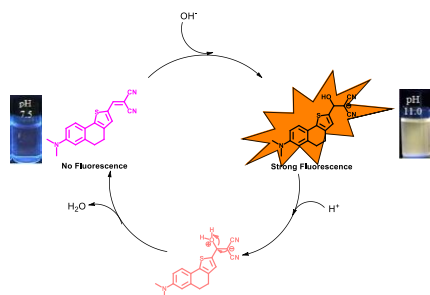


Fig. 6. Proposed mechanism of probe **DDTM** towards pH changes.

To better understand the optical responses of probe **DDTM** upon adding with OH<sup>-</sup>, density functional theory (DFT) calculations were performed using the CAM-B3LYP/6-311+G(d, p) level of Gaussian 09 program [34,35]. The solvent effects were taken into account in water through the polarizable continuum model (PCM) [36]. The optimized structures of **DDTM** and **DDTM-OH<sup>-</sup>** were shown in Fig. 7. The molecular backbone of the **DDTM** was nearly coplanar while the dihedral angle of thiophene ring and dicyanovinyl group in the **DDTM-OH<sup>-</sup>** was 48.9°, indicating the dicyanovinyl group was twisted in response to OH<sup>-</sup>.

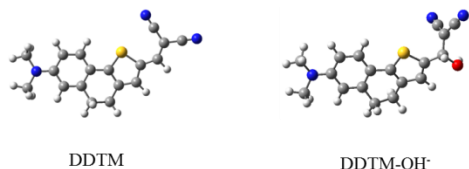


Fig. 7. Optimized structures of **DDTM** and **DDTM-OH<sup>-</sup>** at the CAM-B3LYP/6-311+G(d, p)/PCM theoretical level.

Molecular orbital surfaces of the HOMO and LUMO for compound **DDTM** and **DDTM-OH<sup>-</sup>** were displayed in Fig. 8. For **DDTM**, the electron density in the HOMO was distributed over the whole molecular while that in the LUMO was mainly concentrated on the thiophene ring and dicyanovinyl group, respectively. As for **DDTM-OH<sup>-</sup>**, the electron in HOMO and LUMO orbitals was mostly spread over the moiety of **DTC**. Obviously, there was no ICT process occurred in the **DDTM-OH<sup>-</sup>**, in that a sp<sup>3</sup> hybridized carbon atom existed in vinyl moiety of dicyanomethylidene and dicyanomethylidene twisted. The interruption of the ICT process also resulted in the increased HOMO-LUMO energy gap of **DDTM-OH<sup>-</sup>** (6.39 eV) in comparison with that of the **DDTM** (4.63 eV) and is also

explained for the appearance of a new absorption band at 430 nm in the absorption spectrum of **DDTM-OH<sup>-</sup>**. Therefore, these DFT calculations verified that OH<sup>-</sup> was bound to the vinyl group of probe **DDTM** and are in good agreement with the experimental results.

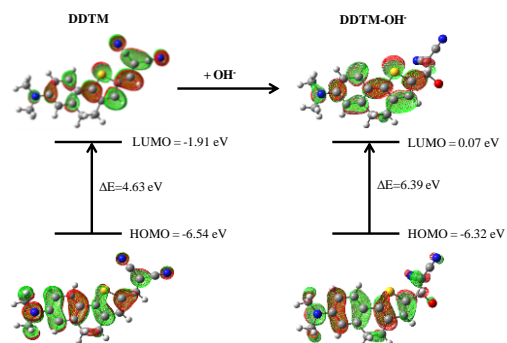


Fig. 8. HOMO-LUMO energy levels and frontier molecular orbitals of probe **DDTM** and the adduct **DDTM-OH<sup>-</sup>**.

### 3.7. Cytotoxicity and fluorescence imaging for living cells

Firstly, the cytotoxic effects of probe **DDTM** were studied in order to evaluate its imaging performance *in vivo*. MTT, a standard cell viability protocol, was employed to evaluate the cytotoxicity of probe **DDTM** on HeLa cells by treating HeLa cells with the probe for 48 h. The probe showed low cytotoxicity and excellent compatibility with more than 80% viability at concentration of 25 μM under experimental conditions (Fig. S3).

Next, the cellular imaging assays were performed to verify whether probe **DDTM** could be applied for determining pH changes in the biological application. HeLa cells were incubated with probe **DDTM** at pH 7.4, 10.0 and 12.0 for 5 min, after that intracellular fluorescence was monitored by confocal microscopy (Fig. 9). Under neutral condition, no fluorescence was observed. On the contrary, moderate fluorescence was observed when cells were incubated with probe **DDTM** at pH 10.0. Furthermore, the strong blue fluorescence was observed at pH 12.0. At the same time, the similar results were obtained in red channel when excitation wavelength was 543 nm. These results indicated that probe **DDTM** displays sensitive fluorescence enhances in a pH-dependent manner in living cells system.

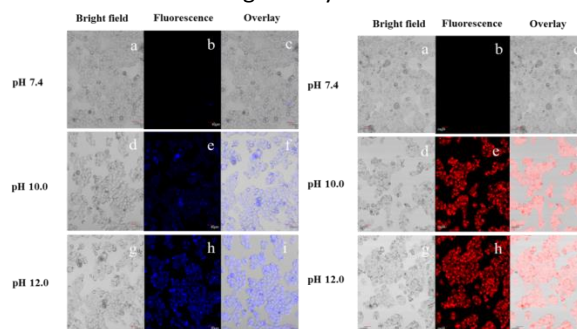
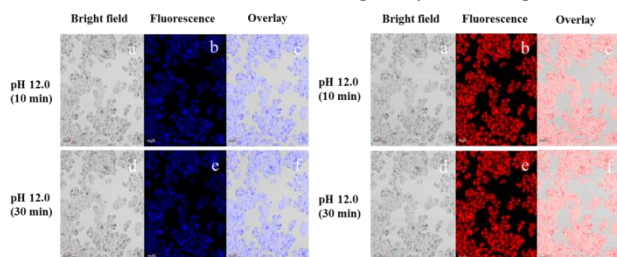


Fig. 9. Confocal fluorescent imaging of HeLa cells incubated with probe **DDTM** (10 μM) at pH 7.4 (a, b, c), 10.0 (d, e, f) and 12.0 (g, h, i),

i) for 5 min, respectively. Left: Excitation wavelength was 405 nm. Right: Excitation wavelength was 543 nm. Scale bar: 40  $\mu$ m.

Additionally, dynamic fluorescence imaging was also occurred to investigate the process of **DDTM** diffusing into cells and the change of fluorescence intensity. As shown in **Fig. 10**, the fluorescence of **DDTM** was obtained at different time-points via confocal laser scanning microscope. After addition of **DDTM** in pH 12.0 alkaline solution, the fluorescence intensity of the HeLa cells had no change and barely any fluorescence quenching was observed until 30 min at 405 nm and 543 nm. These cell experiments demonstrated that probe **DDTM** has excellent stability and biological compatibility in living cells, and could be used to mark the change of pH in living cells.



**Fig. 10.** Dynamic fluorescence images of living HeLa cells on incubation with 10  $\mu$ M **DDTM** for different times 10 min (a, b, c) and 30 min (d, e, f) in pH 12.0 medium. Left: Excitation wavelength was 405 nm. Right: Excitation wavelength was 543 nm. Scale bar: 40  $\mu$ m.

### 3.8. Practical application of probe **DDTM** in pH test strips

In order to further explore the practical application of probe **DDTM**, pH test strips were prepared and utilized to sense different pH according to the excellent properties of probe **DDTM**. The test strip was prepared by immersing filter papers in probe **DDTM** solution (10  $\mu$ M in 20% **DMSO**). After drying in the air, the strip displayed different colour change when the test strips immersed in different pH solution. As shown in **Fig. 11**, the changes of colour in different pH solution were observed in naked eyes and fluorescent light, respectively. Therefore, the distinct colour changes promoted probe **DDTM** to be conveniently used for precise pH paper preparation in real time applications.

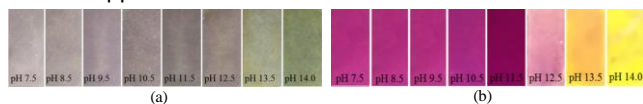


**Fig. 11.** Photographs of colorimetric responses of probe **DDTM** test strips with different pH solutions. (a) Naked eye in visible light. (b) Fluorescence colour changes under 365 nm UV lamp.

## 4. Conclusions

In summary, a novel pH-sensitive colorimetric sensors based on naphthalenone scaffold was designed and synthesized. Probe **DDTM** showed a naked eye visible colour changes from light pink to yellow, and the fluorescence colour was changed

from colourless to orange to yellow in the range pH 9.0-14.0. In addition, the probe exhibited strong pH-dependent behaviour, high selectivity and rapidly respond to pH fluctuations within the range of 9.0 - 14.0. Furthermore, probe **DDTM** displayed a notably large Stokes shift of 198 nm. Live cell imaging data revealed that probe **DDTM** could selectively monitor pH changes with low cytotoxicity and cell membrane permeability. Therefore, the probe could be acted as an effective intracellular pH imaging agent under extreme alkaline conditions in the biomedical and biological fields.

## Conflicts of interest

There are no conflicts of interest to declare.

## Acknowledgements

We sincerely thank the Program for Changjiang Scholars and Innovative Research Team in University (No. IRT\_15R55), the Science Foundation of Northwest University (No. 15NW17), the International Science & Technology Cooperation Program of Shaanxi Province (No. 2016KW-003) and Opening Foundation of Key Laboratory of Resource Biology and Biotechnology in Western China (Northwest University), Ministry of Education.

## Notes and references

- [1] S. C. Burleigh, T. van de Laar, C. J. M. Stroop, W. M. J. van Grunsven, N. O'Donoghue, P. M. Rudd, G. P. Davey, *BMC Biotechnol.*, 2011, **11**, 95-11.
- [2] S. Humez, M. Monet, F. van Coppenolle, P. Delcour, N. Prevarskaya, *Am. J. Physiol. Cell Physiol.*, 2004, **287**, 1733-1746.
- [3] A. L. Edinger, C. B. Thompson, *Curr. Opin. Cell Biol.*, 2005, **16**, 663-669.
- [4] A. C. Johansson, H. Appelqvist, C. Nilsson, K. Kagedal, K. Roberg, K. Ollinger, *Apoptosis.*, 2010, **15**, 527-540.
- [5] V. Estrella, T. Chen, M. Lloyd, J. Wojtkowiak, H. H. Cornell, A. Ibrahim-Hashim, K. Bailey, Y. Balagurunathan, J. M. Rothberg, B. F. Sloane, J. Johnson, R. A. Gatenby, R. J. Gillies, *Cancer Res.*, 2013, **73**, 1524-1535.
- [6] B. A. Webb, M. Chimenti, M. P. Jacobson, D. L. Barber, *Nat. Rev. Cancer.*, 2011, **11**, 671-677.
- [7] T. Myochin, K. Kiyose, K. Hanaoka, H. Kojima, T. Terai, T. Nagano, *J. Am. Chem. Soc.*, 2011, **133**, 3401-3409.
- [8] T. A. Davies, R. E. Fine, R. J. Johnson, C. A. Levesque, W. H. Rathbun, K.F. Seetoo, S.J. Smith, G. Strohmeier, L. Volicer, L. Delva, E.R. Simons, *Biochem. Biophys. Res. Commun.*, 1993, **194**, 537-543.
- [9] S. Harguindey, S. J. Reshkin, G. Orive, J. L. Arranz, E. Anitua, *Curr. Alzheimer Res.*, 2007, **4**, 53-65.
- [10] R. D. Vaughan-Jones, K. W. Spitzer, P. Swietach, Intracellular pH regulation in heart, *J. Mol. Cell. Cardiol.*, 2009, **46**, 318-331.
- [11] W. Dorota, A. Tobias, M. Colette, *Anal. Chem.*, 2014, **86**, 15-29.
- [12] J. Zhou, L. Zhang, Y. Tian, *Anal. Chem.*, 2016, **88**, 2113-2118.
- [13] S. He, R. P. Mason, S. Hunjan, V. D. Mehta, V. Arora, R. Katipally, P. V. Kulkarni, P. P. Antich, *Bioorg. Med. Chem.*, 1998, **6**, 1631-1639.
- [14] L. S. Lawson, J. W. Chan, T. Huser, *Nanoscale.*, 2014, **6**, 7971-7980.
- [15] J. Yin, Y. Hu, J. Yoon, *Chem. Soc. Rev.*, 2015, **44**, 4619-4644.
- [16] C. Dax, M. Coincon, J. Sygusch, C. Blonski, *Biochemistry.*, 2005, **44**, 5430-5443.
- [17] L. W. Lawrence Woo, N. M. Howarth, A. Purohit, H. A. M. Hejaz, M. J. Reed, B. V. L. Potter, *J. Med. Chem.*, 1998, **41**, 1068-1083.
- [18] G. Niu, W. Liu, H. Xiao, H. Zhang, J. Chen, Q. Dai, J. Ge, J. Wu, P. Wang,

- Chem. Asian. J.*, 2015, **11**, 498-504.
- [19] H. Chen, Y. Tang, M. Ren, W. Lin, *Chem. Sci.*, 2016, **7**, 1896-1903.
- [20] N. J. Greco, Y. Tor, *Tetrahedron.*, 2007, **63**, 3515-3527.
- [21] S. C. Rasmussen, S. J. Evenson, C. B. Mccausland, *Chem. Commun.*, 2015, **51**, 4528-4543.
- [22] M. She, S. Wu, Z. Wang, S. Ma, Z. Yang, B. Yin, P. Liu, S. Zhang, J. Li, *Sensor. Actuat. B-Chem.*, 2017, **247**, 129-138.
- [23] X. Jin, S. Wu, M. She, Y. Jia, L. Hao, B. Yin, L. Wang, M. Obst, Y. Shen, Y. Zhang, J. Li, *Anal. Chem.*, 2016, **88**, 11253-11260.
- [24] (a) Z. Liu, X. Wang, Z. Yang, W. He, *J. Org. Chem.*, 2011, **76**, 10286-10290; (b) X. Cheng, Y. Zhou, J. Qin, Z. Li, *ACS. Appl. Mater. Interfaces.*, 2012, **4**, 2133-2138; (c) W. Lin, S. Fang, J. Hu, H. Tsai, K. Chen, *Anal. Chem.*, 2014, **86**, 4648-4652; (d) W. Chen, Z. Zhang, X. Li, H. Agren, J. Su, *RSC Adv.*, 2015, **5**, 12191-12201; (e) J. Orrego-Hernandez, J. Portilla, *J. Org. Chem.*, 2017, **82**, 13376-13385.
- [25] X. Li, Y. Yue, Y. Wen, C. Yin, F. Huo, *Dyes Pigm.*, 2016, **134**, 291-296.
- [26] Y. Ge, P. Wei, T. Wang, X. Cao, D. Zhang, F. Li, *Sensor. Actuat. B-Chem.*, 2018, **254**, 314-320.
- [27] J. Chao, K. Song, H. Wang, Z. Li, Y. Zhang, C. Yin, F. Huo, J. Wang, T. Zhang, *RSC Adv.*, 2017, **7**, 964-970.
- [28] Y. Ge, A. Liu, J. Dong, G. Duan, X. Cao, F. Li, *Sensor. Actuat. B-Chem.*, 2017, **247**, 46-52.
- [29] G. Chen, Q. Fu, F. Yu, R. Ren, Y. Liu, Z. Cao, G. Li, X. Zhao, L. Chen, H. Wang, J. You, *Anal. Chem.*, 2017, **89**, 8509-8516.
- [30] Y. Wen, W. Zhang, T. Liu, F. Huo, C. Yin, *Anal. Chem.*, 2017, **89**, 11869-11874.
- [31] G. Niu, P. Zhang, W. Liu, M. Wang, H. Zhang, J. Wu, L. Zhang, P. Wang, *Anal. Chem.*, 2017, **89**, 1922-1929.
- [32] X. Liu, Y. Su, H. Tian, L. Yang, H. Zhang, X. Song, G. W. Foley, *Anal. Chem.*, 2017, **89**, 7038-7045.
- [33] Y. Ning, J. Cui, Y. Lu, X. Wang, C. Xiao, S. Wu, J. Li, Y. Zhang, *Sensor. Actuat. B-Chem.*, 2018, **269**, 322-330.
- [34] T. Yanai, D. P. Tew, N. C. Handy, *Chem. Phys. Lett.*, 2004, **393**, 51-57.
- [35] C. Lee, W. Yang, R.G. Parr, *Phys. Rev. B.*, 1988, **37**, 85-789.
- [36] J. Tomasi, B. Mennucci, E. Cancès, *J. Mol. Struct.*, (THEOCHEM) 1999, **464**, 211-226.